

Interplay of disorder and magnetic field in the superconducting vortex state

J. Lages,^{1,*} P. D. Sacramento,^{1,†} and Z. Tešanović^{2,‡}

¹ *Centro de Física das Interações Fundamentais,
Instituto Superior Técnico, Av. Rovisco Pais, 1049-001 Lisboa, Portugal*

² *Department of Physics and Astronomy, Johns Hopkins University, Baltimore, Maryland 21218, USA*
(Dated: October 5, 2018)

We calculate the density of states of an inhomogeneous superconductor in a magnetic field where the positions of vortices are distributed completely at random. We consider both the cases of s -wave and d -wave pairing. For both pairing symmetries either the presence of disorder or increasing the density of vortices enhances the low energy density of states. In the s -wave case the gap is filled and the density of states is a power law at low energies. In the d -wave case the density of states is finite at zero energy and it rises linearly at very low energies in the Dirac isotropic case ($\alpha_D = t/\Delta_0 = 1$, where t is the hopping integral and Δ_0 is the amplitude of the order parameter). For slightly higher energies the density of states crosses over to a quadratic behavior. As the Dirac anisotropy increases (as Δ_0 decreases with respect to the hopping term) the linear region decreases in width. Neglecting this small region the density of states interpolates between quadratic and back to linear as α_D increases. The low energy states are strongly peaked near the vortex cores.

PACS numbers: 74.25.Qt, 74.72-h

I. INTRODUCTION

The interaction between the superconductor quasiparticles and the vortices induced by an external magnetic field has been a subject of considerable recent interest^{1,2,3}. In the presence of vortices the quasiparticles feel the combined effect of the external magnetic field and of the spatially varying field of the chiral supercurrents. By performing a gauge transformation to effectively reduce the system to the one in a zero average magnetic field it was shown³ that the natural low energy quasiparticle modes are Bloch waves rather than the Dirac Landau levels proposed in Refs. 1 and 2. The results or Ref.³ also showed that the quasiparticles besides feeling a Doppler shift caused by the moving supercurrents⁴ (Volovik effect) also feel a quantum “Berry” like term due to a half-flux Aharonov-Bohm scattering of the quasiparticles by the vortices.

The effect of disorder on the low-energy density of states of superconductors has also been a subject of much recent activity⁵, particularly in the case of d -wave symmetry. Several conflicting predictions have appeared in the literature which have mainly concentrated on the effect of the presence of impurities. Some progress toward understanding the disparity of theoretical results has been achieved realising that the details of the type of disorder affect significantly the density of states⁵. Particularly in the case of d -wave superconductors, in contrast to conventional gapped s -wave superconductors, the presence of gapless nodes is expected to affect the transport properties. Using a field theoretic description and linearizing the spectrum around the four Dirac-like nodes it has been suggested that the system is critical. It was obtained that the density of states is of the type $\rho(\epsilon) \sim |\epsilon|^\alpha$, where α is a non-universal exponent dependent on the disorder, and that the low energy modes are extended states (critical metal)⁶. Taking into account

the effects of inter-nodal scattering (hard-scattering) it has been shown that an insulating state is obtained instead, where the density of states still vanishes at low energy but with an exponent $\alpha = 1$ independent of disorder⁷. The addition of time-reversal breaking creates two new classes designated spin quantum Hall effect I and II, due to their similarities to the usual quantum Hall effect, corresponding to the hard and soft scattering cases, respectively⁵. The proposed formation of a pairing with a symmetry of the type $d + id$ breaks time-inversion symmetry⁸ but up to now remains a theoretical possibility. On the other hand applying an external magnetic field naturally breaks time-reversal invariance and therefore it is important to study the density of states in this case.

In general, disorder is due to the presence of impurities which may either scatter the quasiparticles and/or may serve as pinning centers for the field induced vortices. The density of states of a dirty but homogeneous s -wave superconductor in a high magnetic field, where the quasiparticles scatter off scalar impurities, was considered using a Landau level basis⁹. For small amounts of disorder it was found that $\rho(\epsilon) \sim \epsilon^2$ but when the disorder is higher than some critical value a finite density of states is created at the Fermi surface. In the same regime of high magnetic fields, but with randomly pinned vortices and no impurities, the density of states at low energies increases significantly with respect to the lattice case suggesting a finite value at zero energy¹⁰. Refs. 11 and 12 considered the effects of random and statistically independent scalar and vector potentials on d -wave quasiparticles and it was predicted¹² that at low energies $\rho(\epsilon) \sim \rho_0 + a\epsilon^2$, where $\rho_0 \sim B^{1/2}$. The effect of randomly pinned *discrete* vortices on the spectrum of a d -wave superconductor was considered recently and a preliminary report was presented in Ref. 13 for the isotropic case. In this work we study the density of states as a function

of vortex density and consider the effects of the Dirac anisotropy. We also study the local density of states (LDOS) and the inverse participation ratio (IPR) and study the effect of disorder on the localization of the low energy states.

The nature of the low energy states in the presence of a single vortex with s -wave symmetry was solved long ago¹⁴. There are localized bound states in the vortex core. The d -wave symmetry case led to some early controversy but it was eventually clearly demonstrated that the low energy states, even though strongly peaked near the vortex core, extend along the four nodal directions and are indeed delocalized as shown by the behavior of IPR¹⁵. In the vortex lattice the states are naturally also extended^{3,16}. In the clean limit it is therefore expected that the external field will increase the low-energy density of states. The expectation that these are delocalized is evidenced by the increase of the thermal conductivity with field¹⁷ in contrast to the reducing effect of conventional superconductors¹⁸.

The addition of impurities in zero magnetic field has been studied using the Bogoliubov-de Gennes (BdG) equations. It was found that the d -wave superconductivity is mainly destroyed locally near a strong scatterer. The superfluid density is strongly suppressed near the impurities but only mildly affected elsewhere¹⁹. No evidence for localization of the low energy states was found and accordingly the superfluid density is indeed suppressed but less than expected^{20,21} and, accordingly, the decrease of the critical temperature with disorder is much slower than previously expected in accordance with experiments²². Similar results of an inhomogeneous order parameter were also obtained for s -wave superconductors²³.

The question we address in this paper is the influence of the positional disorder of the vortices on the quasiparticle states of either a s - or a d -wave superconductor in an external magnetic field and we will not consider the scattering off impurities. We obtain that the low energy states are strongly peaked near the vortex locations as evidenced by the LDOS. At higher energies the states have a very uniform distribution throughout the system. For these states the IPR scales as $1/L^2$ indicative of extended states. In the case of the low energy states the same quantity does not follow this scaling but does not saturate either. This is probably a consequence of finite size effects indicative that the system sizes considered are smaller than the localization length. The results indicate at best a large value for the localization length but are more consistent with extended states rather than with localized states.

In section II we describe the model and present the BdG equations to be solved and consider the effect of the vortices on the supercurrent profiles. In section III we study the effects of positional disorder on s -wave superconductors. In section IV we consider d -wave superconductors for the isotropic and anisotropic cases. Also we study the spatial structure of the low-lying quasipar-

ticle states. We end with the conclusions.

II. DESCRIPTION OF THE MODEL

The strong correlations of the high T_c materials are typically modelled using a Hubbard-like Hamiltonian for the electrons. The superconductivity is considered using a BCS-like formulation which provides good agreement with experimental results. Even though the normal phase of these materials is particularly challenging it is by now accepted that the phenomenology in the superconducting phase is reasonably well described by BCS theory.

A. Bogoliubov-de Gennes Hamiltonian

We will consider the lattice formulation of a disordered d -wave superconductor in a magnetic field. We start from the Bogoliubov-de Gennes equations $\mathcal{H}\psi = \epsilon\psi$ where $\psi^\dagger(\mathbf{r}) = (u^*(\mathbf{r}), v^*(\mathbf{r}))$ and where the matrix Hamiltonian is given by

$$\mathcal{H} = \begin{pmatrix} \hat{h} & \hat{\Delta} \\ \hat{\Delta}^\dagger & -\hat{h}^\dagger \end{pmatrix} \quad (1)$$

with^{3,16}

$$\hat{h} = -t \sum_{\delta} e^{-\frac{ie}{\hbar c} \int_{\mathbf{r}}^{\mathbf{r}+\delta} \mathbf{A}(\mathbf{r}) \cdot d\mathbf{l}} \hat{s}_{\delta} - \epsilon_F \quad (2)$$

and

$$\hat{\Delta} = \Delta_0 \sum_{\delta} e^{\frac{i}{2}\phi(\mathbf{r})} \hat{\eta}_{\delta} e^{\frac{i}{2}\phi(\mathbf{r})}. \quad (3)$$

The sums are over nearest neighbors ($\delta = \pm\mathbf{x}, \pm\mathbf{y}$ on the square lattice); $\mathbf{A}(\mathbf{r})$ is the vector potential associated with the uniform external magnetic field $\mathbf{B} = \nabla \times \mathbf{A}$, the operator \hat{s}_{δ} is defined through its action on space dependent functions, $\hat{s}_{\delta}u(\mathbf{r}) = u(\mathbf{r}+\delta)$, and the operator $\hat{\eta}_{\delta}$ describes the symmetry of the order parameter.

The application of the uniform external magnetic field \mathbf{B} generates in type II superconductors compensating vortices each carrying one half of the magnetic quantum flux, $\frac{\phi_0}{2}$. We take the London limit, which is valid for low magnetic field and over most of the $H-T$ phase diagram in extreme type-II superconductors like the cuprates, assuming that the size of the vortex cores is negligible and placing each vortex core at the center of a plaquette (unit cell). The N_{ϕ} vortices are distributed randomly over the $L \times L$ plaquettes. In this limit we can take the order parameter amplitude Δ_0 constant everywhere in space and we can factorize the phase of the order parameter as shown in Eq. 3.

At this stage, it is convenient to perform a singular gauge transformation to eliminate the phase of the off-diagonal term (3) in the matrix Hamiltonian. We consider the unitary FT gauge transformation $\mathcal{H} \rightarrow \mathcal{U}^{-1}\mathcal{H}\mathcal{U}$,

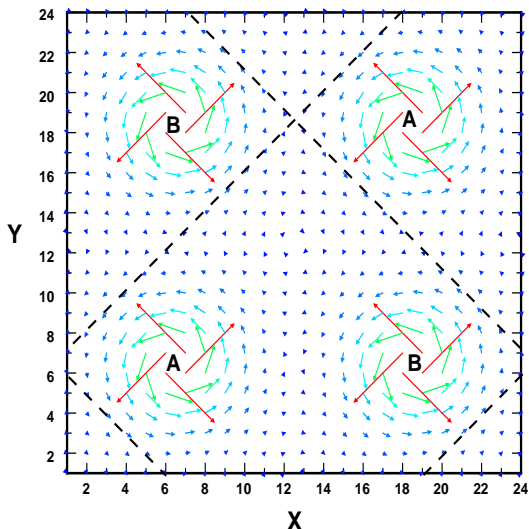


FIG. 1: Color vector field plot showing the profile of the conventional superfluid wave vector $\mathbf{k}_s = \frac{1}{2}(\mathbf{k}_s^A + \mathbf{k}_s^B)$ for a regular vortex lattice and for $B = 1/144$.

where³

$$\mathcal{U} = \begin{pmatrix} e^{i\phi_A(\mathbf{r})} & 0 \\ 0 & e^{-i\phi_B(\mathbf{r})} \end{pmatrix} \quad (4)$$

with $\phi_A(\mathbf{r}) + \phi_B(\mathbf{r}) = \phi(\mathbf{r})$. The phase field $\phi(\mathbf{r})$ is then decomposed at each site of the two-dimensional lattice in two components $\phi_A(\mathbf{r})$ and $\phi_B(\mathbf{r})$ which are assigned respectively to a set of vortices A , positioned at $\{\mathbf{r}_i^A\}_{i=1, N_A}$, and a set of vortices B , positioned at $\{\mathbf{r}_i^B\}_{i=1, N_B}$. The phase fields $\phi_{\mu=A,B}$ are naturally defined through the equation

$$\nabla \times \nabla \phi_\mu(\mathbf{r}) = 2\pi\mathbf{z} \sum_i \delta(\mathbf{r} - \mathbf{r}_i^\mu) \quad (5)$$

where the sum runs only over the μ -type vortices. After carrying out the gauge transformation (4) the Hamiltonian (1) reads

$$\mathcal{H}' = \begin{pmatrix} -t \sum_{\delta} e^{i\mathcal{V}_{\delta}^A(\mathbf{r})} \hat{s}_{\delta} - \epsilon_F & \Delta_0 \sum_{\delta} e^{-i\frac{\delta\phi}{2}} \hat{\eta}_{\delta} e^{i\frac{\delta\phi}{2}} \\ \Delta_0 \sum_{\delta} e^{-i\frac{\delta\phi}{2}} \hat{\eta}_{\delta}^{\dagger} e^{i\frac{\delta\phi}{2}} & t \sum_{\delta} e^{-i\mathcal{V}_{\delta}^B(\mathbf{r})} \hat{s}_{\delta} + \epsilon_F \end{pmatrix}. \quad (6)$$

The phase factors are given by¹⁶ $\mathcal{V}_{\delta}^{\mu}(\mathbf{r}) = \int_{\mathbf{r}}^{\mathbf{r}+\delta} \mathbf{k}_s^{\mu} \cdot d\mathbf{l}$ and $\delta\phi(\mathbf{r}) = \phi_A(\mathbf{r}) - \phi_B(\mathbf{r})$, where $\hbar\mathbf{k}_s^{\mu} = m\mathbf{v}_s^{\mu} = \hbar\nabla\phi_{\mu} - \frac{e}{c}\mathbf{A}$ is the superfluid momentum vector for the μ -supercurrent. Physically, the vortices A are only visible to the particles and the vortices B are only visible to the holes. Each resulting μ -subsystem is then in an effective magnetic field

$$\mathbf{B}_{\text{eff}}^{\mu} = -\frac{mc}{e}\nabla \times \mathbf{v}_s^{\mu} = \mathbf{B} - \phi_0\mathbf{z} \sum_i \delta^2(\mathbf{r} - \mathbf{r}_i^{\mu}) \quad (7)$$

where each vortex carries now an effective quantum magnetic flux ϕ_0 . For the case of a regular vortex lattice^{3,16},

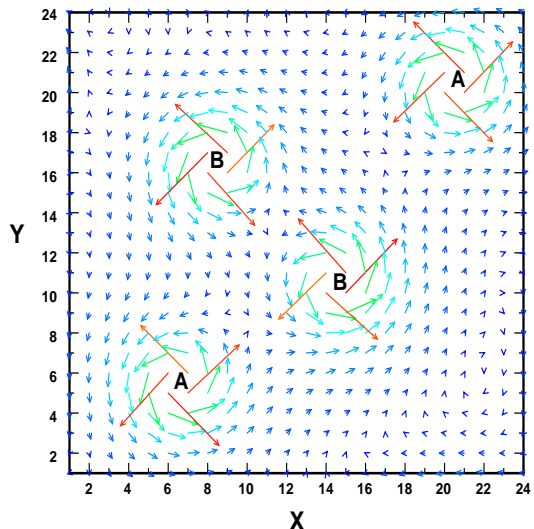


FIG. 2: Color vector field plot showing the profile of the conventional superfluid wave vector $\mathbf{k}_s = \frac{1}{2}(\mathbf{k}_s^A + \mathbf{k}_s^B)$ for a random configuration of vortices and for $B = 1/144$.

these effective magnetic fields vanish simultaneously on average if the magnetic unit cell contains two vortices, one of each type. More generally, in the absence of spatial symmetries, as it is the case for disordered systems, these effective magnetic fields $\mathbf{B}_{\text{eff}}^{\mu=A,B}$ vanish if the numbers of vortices of the two types A and B are equal, i.e. $N_A = N_B$, and their sum equals to the number of elementary quantum fluxes of the external magnetic field penetrating the system. As the number of vortices N_{ϕ} in the two-dimensional system of size $L \times L$ is proportional to the quantized magnetic flux piercing through the system, we choose to parametrize the magnetic field intensity by the ratio of the number of vortices, $N_{\phi} = N_A + N_B$, by the number of lattice sites, $B = \frac{N_{\phi}}{L \times L}$.

We consider here the disorder induced by the random pinning of the N_{ϕ} vortices over the two-dimensional $L \times L$ lattice. As the effective magnetic fields (7) experienced by the particles and the holes vanish on average within the gauge transformation (4) we are allowed to use periodic boundary conditions on the square lattice ($\Psi(x+nL, y) = \Psi(x, y+mL) = \Psi(x, y)$ with $n, m \in \mathbb{Z}$). The $L \times L$ original lattice becomes then a magnetic supercell where the vortices are placed at random with a mean intervortex spacing $\ell = 1/\sqrt{B}$. The disorder in the system is then established over a length L .

In order to compute the eigenvalues and eigenvectors of the Hamiltonian (6) we seek for eigensolutions in the Bloch form $\Psi_{n\mathbf{k}}^{\dagger}(\mathbf{r}) = e^{-i\mathbf{k}\cdot\mathbf{r}}(U_{n\mathbf{k}}^*, V_{n\mathbf{k}}^*)$ where \mathbf{k} is a point of the Brillouin zone. In the following we will label these eigensolutions with the index $\mathbf{n} = (n, \mathbf{k})$. We diagonalize then the Hamiltonian $e^{-i\mathbf{k}\cdot\mathbf{r}}\mathcal{H}'e^{i\mathbf{k}\cdot\mathbf{r}}$ for a large number of points \mathbf{k} in the Brillouin zone and for many different realizations (around 100) of the random vortex pinning. The results of these computations are shown in section III for the s -wave disordered superconductor case and in

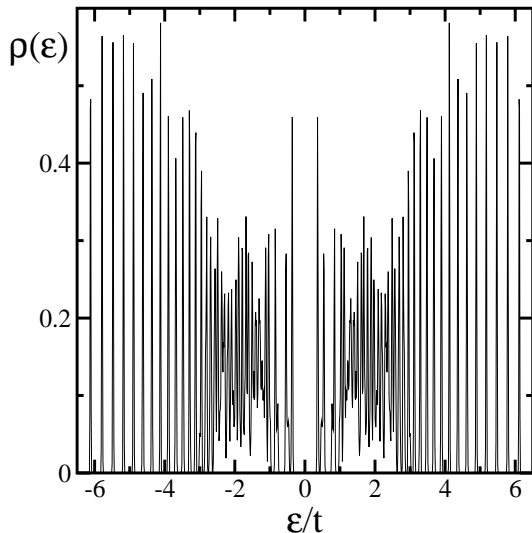


FIG. 3: Quasiparticle density of states for the s -wave symmetry and for a regular lattice of vortices (no disorder). The magnetic field is $B = 1/18$, the magnetic unit cell contains 2 vortices piercing an area of 6×6 . The parameters are $\mu = -2.2t$ and $\Delta_0 = t$.

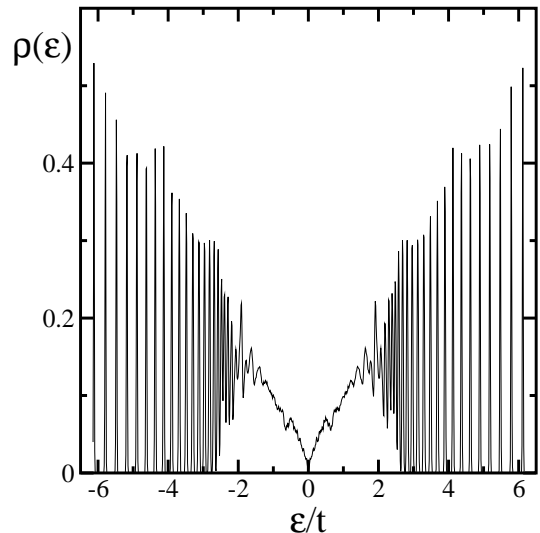


FIG. 4: Quasiparticle density of states for the s -wave symmetry and for a disordered lattice of vortices. The magnetic field is $B = 1/18$ and the linear system size is $L = 18$. The parameters are $\mu = -2.2t$ and $\Delta_0 = t$.

section IV for the d -wave disordered superconductor case.

B. Profiles of supercurrents

The μ -superfluid wave vector $\mathbf{k}_s^\mu(\mathbf{r})$ characterizes the supercurrents induced by the μ -vortices. This vector can be calculated for an arbitrary configuration of vortices¹⁶ like

$$\mathbf{k}_s^\mu(\mathbf{r}) = 2\pi \int \frac{d^2k}{(2\pi)^2} \frac{i\mathbf{k} \times \mathbf{z}}{k^2 + \lambda^{-2}} \sum_{i=1}^{\infty} e^{i\mathbf{k} \cdot (\mathbf{r} - \mathbf{r}_i^\mu)}. \quad (8)$$

Here λ is the magnetic penetration length and the sum extends over the infinite number of μ -type vortex positions. We consider the case $\lambda \rightarrow \infty$ which is an excellent approximation in extreme type-II systems like high temperature superconductors. In this limit the repulsive interaction between vortices is not screened and therefore the vortex distribution is not strictly arbitrary – long range interactions will try to force the vortex system to take only incompressible configurations. For the purposes of this paper, we assume that the pinning centers are strong enough to overcome the vortex repulsion over the lengthscales relevant to experiments. Thus, we are considering the limit of strong pinning. We have checked that the case with a random distribution of vortices is qualitatively the same as for the case where the vortex positions are allowed to vary with a radius of a few unit cells around a regular lattice position.

The μ -superfluid wave vector distribution is completely determined by the configuration of the μ -vortices, as can be seen from Eq. 8 and is independent of the pairing symmetry. Since we are taking the London limit, where

the vortex core size is negligible, we neglect any possible different symmetry contributions from inside the vortex core²⁴ and the chiral supercurrents simply reflect the circulation of the superfluid density around the vortex.

In order to compute efficiently the μ -superfluid wave vector we use the translational symmetry introduced by the periodic repetition of the $L \times L$ supercells and then we are able to use the Fourier series representation of expression (8), e.g.

$$\mathbf{k}_s^\mu(\mathbf{r}) = \frac{2i\pi}{(L\delta)^2} \sum_{\mathbf{Q} \neq 0} \frac{\mathbf{Q} \times \mathbf{z}}{Q^2} \sum_{i=1}^{N_\mu} e^{i\mathbf{Q} \cdot (\mathbf{r} - \mathbf{r}_i^\mu)} \quad (9)$$

where $\mathbf{Q} = \frac{2\pi}{L\delta} (n_1, n_2)$ with $n_1, n_2 \in \mathbb{Z}$. We remark that the sum over vortex positions runs now only over the μ -type vortices within a supercell and not, as in Eq. 8, over the infinite number of μ -type vortices present in the two-dimensional system. The price to pay for this procedure is the preceding infinite sum over the reciprocal vectors \mathbf{Q} . We truncate this latter sum when the convergence of each components of $\mathbf{k}_s^\mu(\mathbf{r})$ in each lattice point \mathbf{r} is attained.

Figures 1 and 2 show examples of distributions of the conventional superfluid wave vector which is half the sum of the two types of superfluid wave vector,

$$\mathbf{k}_s(\mathbf{r}) = \frac{\mathbf{k}_s^A(\mathbf{r}) + \mathbf{k}_s^B(\mathbf{r})}{2} = \frac{1}{2} \nabla \phi - \frac{e}{c} \mathbf{A}. \quad (10)$$

In Fig. 1 we show the profile of the supercurrent velocities in the lattice case. The unit cell has two vortices, one of each type A and B . In Figure 2 we show the supercurrents for an arbitrary configuration of the vortices. For example, the 24×24 lattice shown in Fig. 2 can illustrate a disordered supercell corresponding to a magnetic

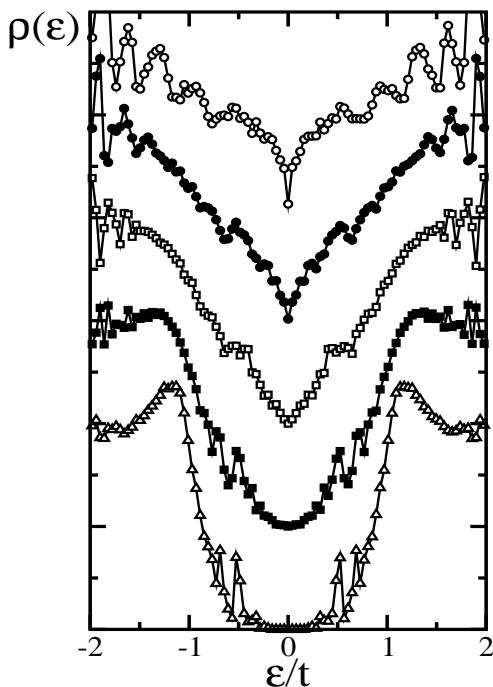


FIG. 5: Quasiparticle density of states (*s*-wave) for different magnetic fields $B = 2/200$ (\triangle), $B = 4/200$ (\blacksquare), $B = 7/200$ (\square), $B = 11/200$ (\bullet) and $B = 20/200$ (\circ) in units of $hc/(2e\delta^2)$. The linear system size is $L = 20$ and the parameters are $\mu = -2.2t$, $\Delta_0 = t$. For clarity the different curves are vertically shifted.

field $B = 1/144$ with two *A*-type vortices and two *B*-type vortices. As it should be, the labelling of the *A*- and the *B*-type vortices is completely arbitrary. The intensity of the supervelocities for the regular and the disordered vortex lattice peak around each vortex and decrease rapidly outside the vicinity of the vortex core ($\sim 5\delta$).

III. DISORDERED *s*-WAVE SUPERCONDUCTORS

For the conventional *s*-wave case the operator characterizing the symmetry of the order parameter is constant $\hat{\eta}_\delta = \frac{1}{4}$ and the off-diagonal terms of the Hamiltonian (6) are then considerably simplified

$$\mathcal{H}' = \begin{pmatrix} -t \sum_{\delta} e^{i\mathcal{V}_\delta^A(\mathbf{r})} \hat{s}_\delta - \epsilon_F & \Delta_0 \\ \Delta_0 & t \sum_{\delta} e^{-i\mathcal{V}_\delta^B(\mathbf{r})} \hat{s}_\delta + \epsilon_F \end{pmatrix}. \quad (11)$$

The *s*-wave Hamiltonian (11) describes coupled particles and holes evolving each in an effective magnetic field composed by the external magnetic field and the counteracting field of ϕ_0 flux carrying vortices. The effective magnetic fields are characterized by the Peierls phase factors $\mathcal{V}_\delta^{\mu=A,B}$. Independently of the system being disordered

or not, the tails of the quasiparticles spectrum ($\epsilon \gg \Delta_0$) are expected to be described by quantized Landau levels.

In Fig. 3 we show the density of states for a field $B = 1/18$ in the case of no disorder. The gap is clearly seen at low energies characteristic of *s*-wave symmetry. The states inside the gap (for $|\epsilon| < t$ in Fig. 3) are the typical Caroli - de Gennes - Matricon (CdGM) bound states¹⁴. At higher energies the Landau levels are clearly visible.

In Fig. 4 we show the effects of disorder for the same *B* field in a lattice of 18×18 sites (18 vortices). The gap is filled by the disorder. The reader should observe here that our disorder is in certain sense “infinite” since we place vortex positions completely at random. Thus, it appears that such full randomness in vortex positions, generated by strong pinning, suffices to close the gap in the single particle density of states. In contrast, the Landau level quantization structure clearly persists at high excitation energies. In general the increase of the magnetic field modifies the curvature of the quasiparticle density of states for the low energies. As it is shown in Fig. 5 the density of states seems to be described by the power-law formula

$$\rho(\epsilon) \sim \epsilon^\alpha. \quad (12)$$

In Fig. 6 we fit the magnetic field dependence of the exponent α . This exponent obeys the following law

$$\alpha \simeq c\ell - d \quad (13)$$

where $\ell = 1/\sqrt{B}$ is the mean intervortex spacing and d is found close to 1. In the cases of a strong magnetic field the density of vortices is high and strictly we are in a regime where the size of the vortex cores can not be neglected. In this regime the Landau level structure at high energies is clear and it extends to low energies superimposed by the effects of disorder. The lower limit for this high magnetic field regime is the value $B \simeq 0.16$ for which $\alpha = 0$ in Fig. 6.

IV. DISORDERED *d*-WAVE SUPERCONDUCTORS

For the unconventional *d*-wave case the operator $\hat{\eta}_\delta$ takes the form $\hat{\eta}_\delta = (-1)^{\delta_y} \hat{s}_\delta$, we recall that \hat{s}_δ acts on spatial dependent functions as $\hat{s}_\delta u(\mathbf{r}) = u(\mathbf{r} + \delta)$ and that $\delta = \pm\mathbf{x}, \pm\mathbf{y}$ characterizes unit displacements (hops) on the lattice. With these definitions the *d*-wave Hamiltonian can be derived from the Hamiltonian (6) and reads

$$\mathcal{H}' = \begin{pmatrix} -t \sum_{\delta} e^{i\mathcal{V}_\delta^A(\mathbf{r})} \hat{s}_\delta - \epsilon_F & \Delta_0 \sum_{\delta} e^{i\mathcal{A}_\delta(\mathbf{r}) + i\pi\delta_y} \hat{s}_\delta \\ \Delta_0 \sum_{\delta} e^{-i\mathcal{A}_\delta(\mathbf{r}) - i\pi\delta_y} \hat{s}_\delta & t \sum_{\delta} e^{-i\mathcal{V}_\delta^B(\mathbf{r})} \hat{s}_\delta + \epsilon_F \end{pmatrix} \quad (14)$$

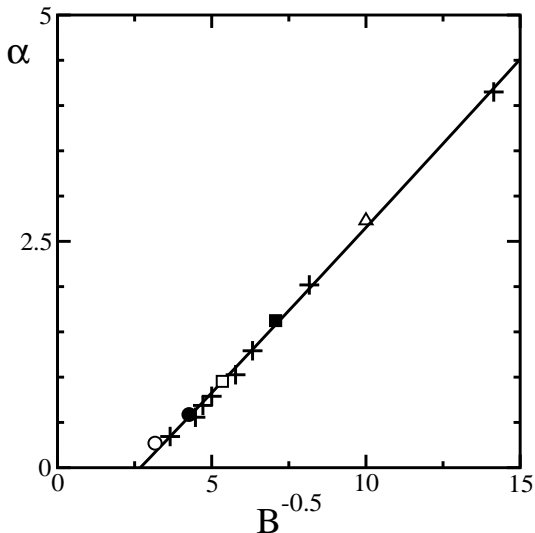


FIG. 6: Magnetic field dependence of the exponent α extracted from the power-law fit $\rho(\epsilon) \sim \epsilon^\alpha$ of the data presented in Fig. 5. The symbols (Δ), (\blacksquare), (\square), (\bullet) and (\circ) denote the same values of B as in Fig.5; the symbols (+) denote others values of B not presented in Fig.5.

where the phase factor $\mathcal{A}_\delta(\mathbf{r})$ has the form

$$\begin{aligned} \mathcal{A}_\delta(\mathbf{r}) &= \frac{1}{2} \int_{\mathbf{r}}^{\mathbf{r}+\delta} (\nabla\phi_A - \nabla\phi_B) \cdot d\mathbf{l} \\ &= \frac{1}{2} \int_{\mathbf{r}}^{\mathbf{r}+\delta} (\mathbf{k}_s^A - \mathbf{k}_s^B) \cdot d\mathbf{l}. \end{aligned} \quad (15)$$

In the Hamiltonian (14) and in Eq. 15 the vector

$$\mathbf{a}_s = \frac{1}{2} (\mathbf{k}_s^A - \mathbf{k}_s^B) \quad (16)$$

acts as an internal gauge field independent of the external magnetic field¹⁶. The associated internal magnetic field $\mathbf{b} = \nabla \times \mathbf{a}_s$ consists of opposite $A - B$ spikes fluxes carrying each one half of the magnetic quantum flux ϕ_0 , centered in the vortex cores and vanishing on average since the numbers of A - and B -type vortices are the same.

A. Differences from the regular vortex lattice case

The situation where the vortices are regularly distributed in a lattice was treated before¹⁶. Since the average effective magnetic field vanishes it is possible to solve the BdG equations using a standard Bloch basis— the supercurrent velocities are periodic in space and there is no need to consider the magnetic Brillouin zone. Taking the continuum limit and linearizing the spectrum around each node effectively decouples the nodes. It was shown that the low-energy quasiparticles are then naturally described as Bloch waves³ and not Dirac-Landau levels as previously proposed^{1,2}. However, it was found that in the linearized problem different assignments of the A and B

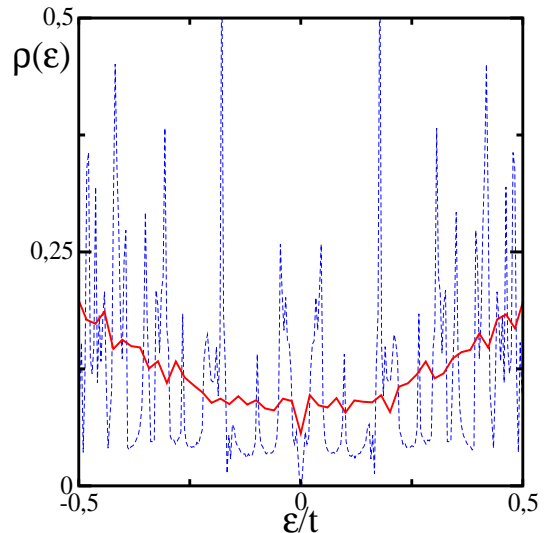


FIG. 7: Quasiparticle density of states for the d -wave case without (dashed line) and with disorder (solid line). The intensity of the magnetic field is $B = 1/121$, $\Delta = 0.5t$, $\mu = -2.2t$ and the linear system size is $L = 22$.

vortices lead to somewhat different spectra, which was unexpected¹⁶. It was found that defining theory on the lattice regularized this problem and indeed the system has a manifest internal gauge symmetry such that the spectrum is independent of the A - B vortex assignments, as it should be. Moreover, the lattice formulation explicitly involves internodal contributions which are important for the properties of the density of states in the disordered case. In the vortex lattice case, however, it was found that only in special commensurate cases (for the square lattice) the inclusion of the internodal contributions is relevant since only in such cases a gap develops due to the interference terms between the various nodes, estimated to be of the order of \sqrt{B} . In a general incommensurate case the interference is not relevant leading to qualitatively similar spectra. In the d -wave case the spectrum is gapless with a linear density of states at low energy¹⁶. One would therefore expect that in a general disordered vortex case internodal scattering might not be relevant (particularly for high Dirac cone anisotropy $\alpha_D = v_F/v_\Delta = t/\Delta_0 \gg 1$).

In Fig. 7 we compare the densities of states for the lattice case and a case with disorder. At weak fields the density of states is small at low energies having a dip close to zero energy. We have checked for finite size effects on the spectrum. For system sizes larger than 16×16 the density of states at not very low energies converges and the finite size dependence is negligible.

B. Isotropic case

In this subsection we will focus our attention on the isotropic case $\alpha_D = 1$ in order to extract the general

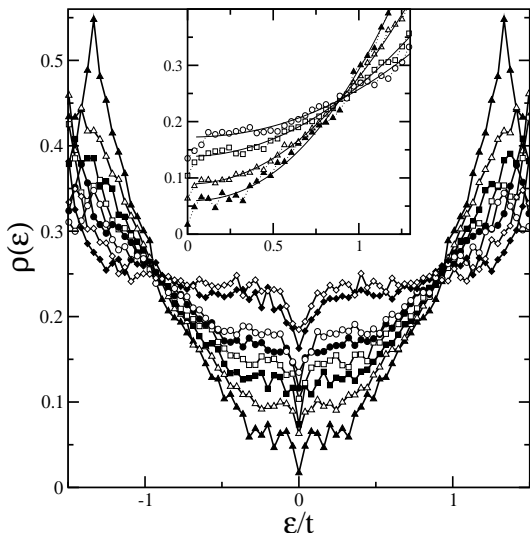


FIG. 8: Quasiparticle density of states for the d -wave case and for different magnetic fields $B = 1/200$ (\blacktriangle), $B = 3/200$ (\triangle), $B = 5/200$ (\blacksquare), $B = 7/200$ (\square), $B = 9/200$ (\bullet), $B = 11/200$ (\circ), $B = 20/200$ (\blacklozenge) and $B = 25/200$ (\diamond) in units of $hc/(2e\delta^2)$. The linear system size is $L = 20$ and the parameters are $\mu = -2.2t$, $\Delta_0 = t$. The inset shows the fits of the density of states (solid lines) inside the presented energy interval. For clarity not all the fits are shown.

dependencies of the quasiparticle density of states in the magnetic field B .

In Fig. 8 we show the density of states for a system with size 20×20 and for various magnetic fields. The density of states at small energies is finite up to quite small energies where there is a dip to a value that decreases as the magnetic field decreases. Only for quite small magnetic fields the density of states approaches zero at the origin. Neglecting the narrow region close to the origin we have fitted the density of states using the power law

$$\rho(\epsilon) = \rho_0 + \beta|\epsilon|^\alpha. \quad (17)$$

In the inset of Fig. 8 we show the fits for the various values of the magnetic field. Reasonable fits are obtained taking $\alpha \sim 2$ and we obtain that $\rho_0 \sim B^{1/2}$. The various system sizes fit in the same universal curve indicating that the finite size effects are negligible. Note that in the lattice case the density of states at low energies is linear^{3,16,25,26} (this result differs from the behavior obtained by others for a d -wave superconductor with no disorder^{4,27}, where $\rho(\epsilon \sim 0) \sim B^{1/2}$). The finite density of states at zero energy is therefore a consequence of finite disorder.

In Fig. 9 we focus on the narrow region close to $\epsilon = 0$ for the same set of parameters considered in Fig. 8. Except for the lowest field case $B = 1/200$ the density of states seems to be finite at zero energy. Here the field density $B = 1/200$ corresponds to the particular case where only two vortices pierced the 20×20 disordered supercell. As shown in Ref. 25 in this case the spectrum

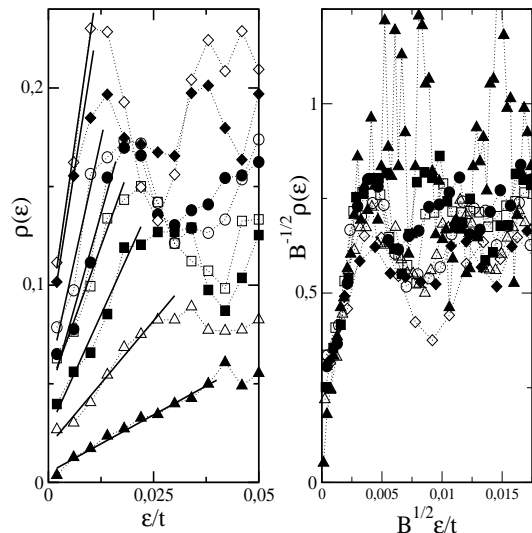


FIG. 9: Low-energy quasiparticle density of states $\rho(\epsilon)$ for the d -wave case and for different magnetic field $B = 1/200$ (\blacktriangle), $B = 3/200$ (\triangle), $B = 5/200$ (\blacksquare), $B = 7/200$ (\square), $B = 9/200$ (\bullet), $B = 11/200$ (\circ), $B = 20/200$ (\blacklozenge) and $B = 25/200$ (\diamond) in unit of $hc/(2e\delta^2)$. For each data sets the linear system size is $L = 20$, the same as in Fig. 8. In the left panel the solid lines are linear fits of the dip region below $\epsilon = 0.02t$ of the type $\rho(\epsilon) = \rho_{0\text{dip}} + \beta|\epsilon|$. In the right panel we present the near scaling at low energies (see text).

is usually gapped and therefore the density of states vanishes at zero energy. Performing a fit like in Eq. 17 we obtain an exponent which is now close to 1. In this regime $\rho_{0\text{dip}}$ also scales with \sqrt{B} and the slope scales linearly with B . In this low energy regime the finite size effects are still noticeable but the dependence on the magnetic field is common to the various system sizes. At these low energies the density of states for the various system sizes appears to be of the following approximate form

$$\rho(\epsilon) \sim \frac{1}{\omega_H} \frac{1}{l^2} \mathcal{F} \left(\frac{\epsilon}{\omega_H} \frac{\delta^2}{l^2} \right), \quad (18)$$

where $\omega_H \sim \sqrt{\Delta B}$ and \mathcal{F} is a universal function. In the left panel of Fig. 9 we show $\rho(\epsilon)$ for various fields while in the right panel we illustrate the near scaling at low energies consistent with $\mathcal{F}(x) \sim c_1 + c_2x$ at small x . Note that $\beta(B \rightarrow 0)$ appears to be small but finite, consistent with a crossover to a “Dirac node” scaling $\rho(\epsilon) \sim (1/\omega_H)(1/l^2)\mathcal{F}(\epsilon/\omega_H)$ at very low fields.

C. Anisotropic case

We investigate now the dependence of the quasiparticle density of state on the value of the Dirac anisotropy ratio α_D . Such a study is interesting in order to compare our results with experiments; indeed for high- T_c superconductors such as $\text{YBa}_2\text{Cu}_3\text{O}_7$ and $\text{Bi}_2\text{Sr}_2\text{CaCu}_2\text{O}_8$ the

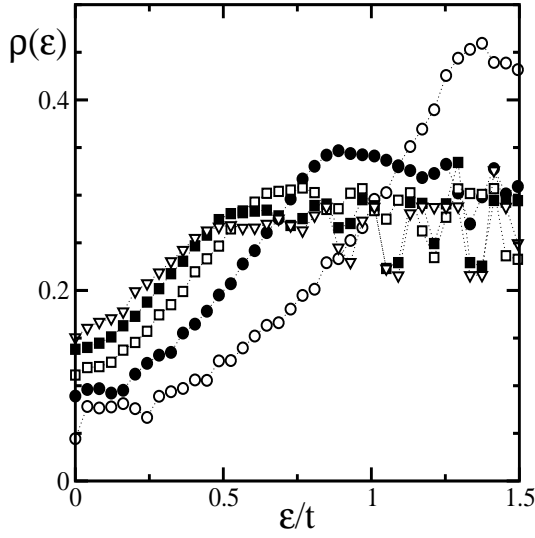


FIG. 10: Quasiparticle density of states for the d -wave case for different values of the anisotropy parameter: $\alpha_D = 1$ (\circ), $\alpha_D = 2$ (\bullet), $\alpha_D = 3$ (\square), $\alpha_D = 4$ (\blacksquare) and $\alpha_D = 5$ (∇). The magnetic field intensity is $B = 1/100$. The linear system size is $L = 20$ and the chemical potential is $\mu = -2.2t$.

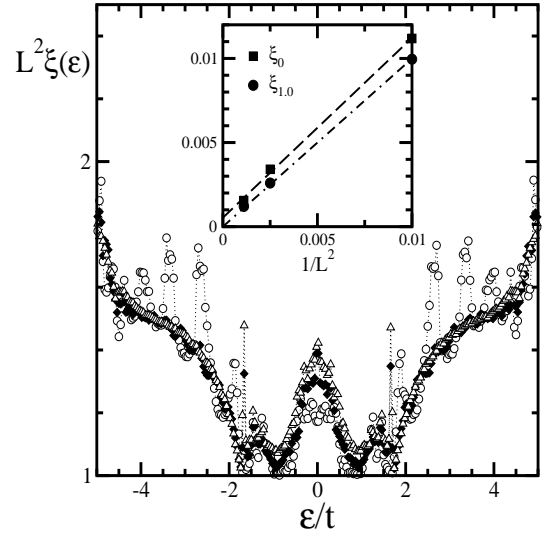


FIG. 12: Inverse participation ratio ξ as a function of the quasiparticle energy ϵ for $B = 1/25$ and for different linear system sizes $L = 10$ (\circ), $L = 20$ (\blacklozenge) and $L = 30$ (\triangle). Inset: scaling of the inverse participation ratio with $1/L^2$ for states in the close vicinity of the Fermi surface $|\epsilon| \leq 0.05t$ (ξ_0 , \blacksquare) and for states with energy $|\epsilon| \simeq t$ ($\xi_{1.0}$, \bullet).

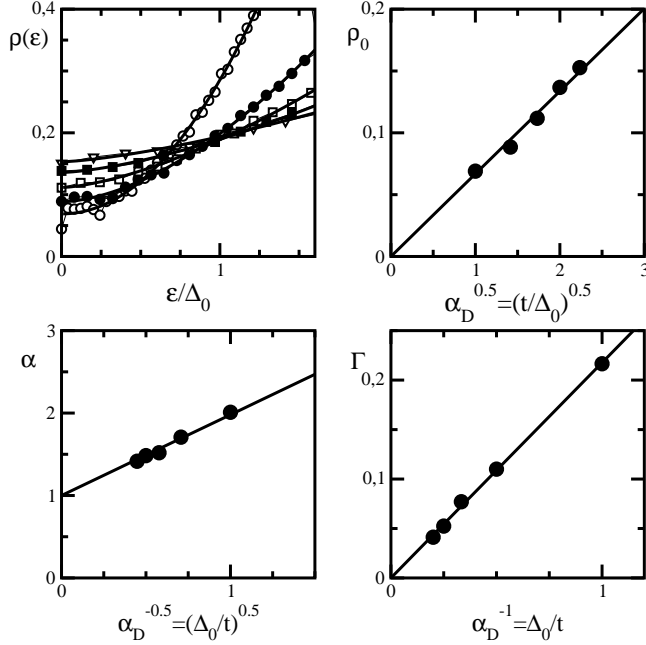


FIG. 11: Fits of the data presented in Fig. 10. Upper left panel: quasiparticle density of states presented in Fig. 10 (the same symbols are used) as a function of the rescaled energy ϵ/Δ_0 . Solid lines are fits of the power law type $\rho(\epsilon) = \rho_0 + \Gamma (\epsilon/\Delta_0)^\alpha$. On the others panel solid lines are linear fits. Upper right panel: zero energy quasiparticle density of states ρ_0 as a function of $\sqrt{\alpha_D}$. Lower left panel: Power law exponent α as a function of $1/\sqrt{\alpha_D}$. Lower right panel: Parameter Γ of the power law as a function of $1/\alpha_D$.

Dirac anisotropy ratio is^{17,28} respectively $\alpha_D \simeq 14$ and $\alpha_D \simeq 19$.

In the lattice case a high anisotropy increases the density of states at low energies and leads to lines of quasi-nodes^{16,25}. At high anisotropy ($\Delta_0 \ll t$) the nodes are very narrow and a one-dimensional like character is evidenced.

As shown in Fig. 10, the low-energy quasiparticle density of states at constant field is filled when the anisotropy parameter α_D is increased. There is a narrow linear region close to the origin that decreases as α_D increases. Fig. 11 shows the power law fits of the data presented in Fig. 10 neglecting a very narrow region of width $\sim 0.025t$ around $\epsilon = 0$. It turns out that the low-energy quasiparticle density of states has the form

$$\rho(\epsilon) \sim \rho_0 + \Gamma \left(\frac{\epsilon}{\Delta_0} \right)^\alpha \quad (19)$$

with zero-energy density of states

$$\rho_0 \sim \sqrt{\frac{t}{\Delta_0}}, \quad (20)$$

the exponent

$$\alpha \simeq 1 + \sqrt{\frac{\Delta_0}{t}} \quad (21)$$

and the parameter

$$\Gamma \sim \frac{\Delta_0}{t}. \quad (22)$$

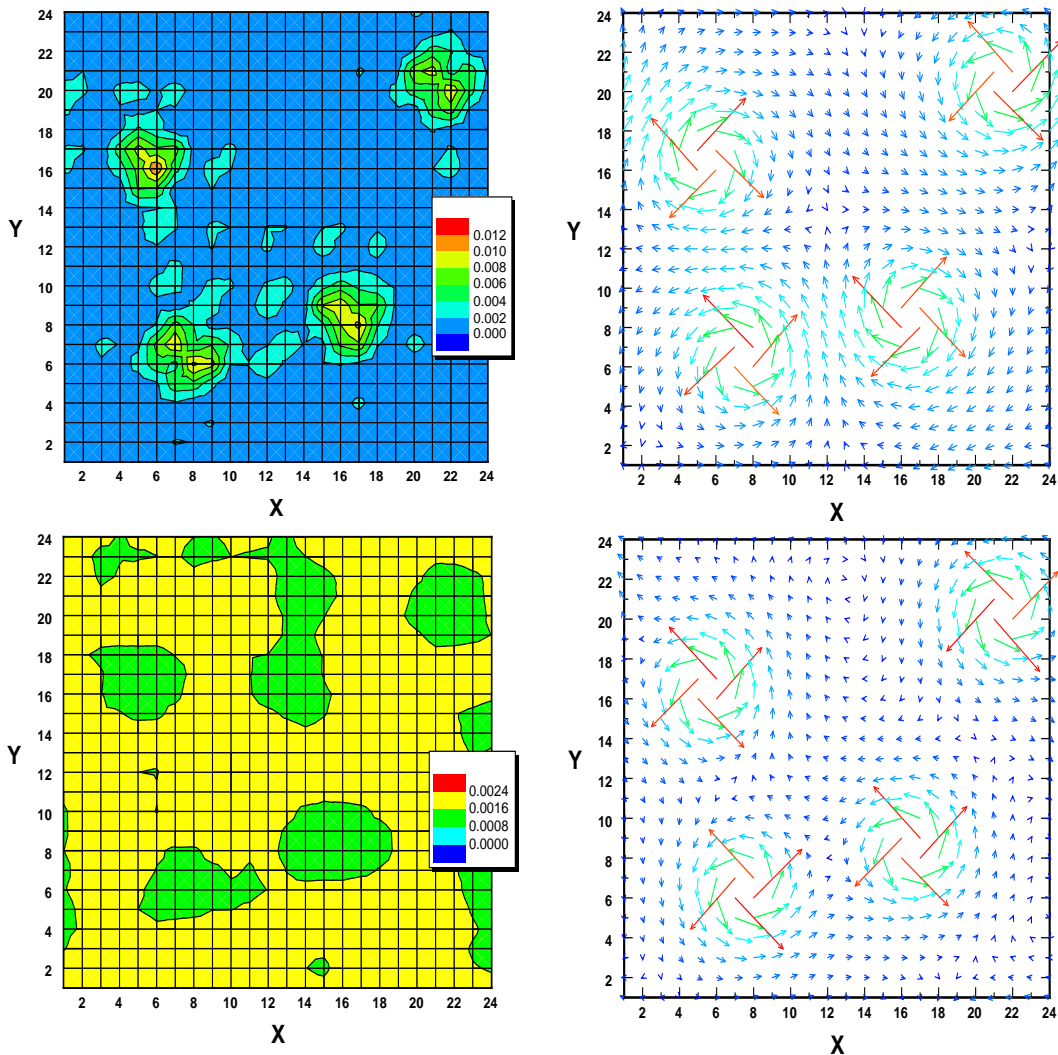


FIG. 13: Upper left panel: Color density plot of the quasiparticle local density of states $\rho(\mathbf{r}, \epsilon)$ for $\epsilon \simeq 0$. Lower left panel: Color density plot of the quasiparticle local density of states $\rho(\mathbf{r}, \epsilon)$ for $\epsilon \simeq t$. Upper right panel: Color vector field plot showing the profile of the internal gauge field $\mathbf{a}_s = \frac{1}{2}(\mathbf{k}_s^A - \mathbf{k}_s^B)$. Lower right panel: Color vector field plot showing the profile of the conventional superfluid wave vector $\mathbf{k}_s = \frac{1}{2}(\mathbf{k}_s^A + \mathbf{k}_s^B)$. All the panels correspond to the same configuration of the vortex pinning and to the same magnetic field $B = 1/144$.

The dependence of the exponent is interesting since in the isotropic case we retrieve $\alpha = 2$ and with increasing anisotropy the exponent decreases to 1 (see lower left panel of Fig. 11) characteristic of the Dirac nodes. At $\epsilon \simeq 0$ and for a high Dirac anisotropy ratio the quasiparticle density of states flattens since the coefficient Γ in (19) decreases with Δ_0 .

D. Spatial structure of the low-lying quasiparticle states

As discussed above, the nature of the low lying states is an important point which is relevant due to the presence of disorder. A standard way to analyse the nature of the states is to study the IPR. The IPR is defined in the

usual way

$$\xi(\epsilon) = \frac{\left\langle \sum_{\mathbf{n}, \mathbf{r}} (|u_{\mathbf{n}}(\mathbf{r})|^4 + |v_{\mathbf{n}}(\mathbf{r})|^4) \delta(\epsilon - E_{\mathbf{n}}) \right\rangle}{\left\langle \sum_{\mathbf{n}, \mathbf{r}} (|u_{\mathbf{n}}(\mathbf{r})|^2 + |v_{\mathbf{n}}(\mathbf{r})|^2) \delta(\epsilon - E_{\mathbf{n}}) \right\rangle^2}. \quad (23)$$

The brackets denote the averaging over disorder configurations. The IPR ξ is a direct measure of the spatial extend of the quasiparticle wavefunctions. It scales as $1/L^2$ for extended states and is constant for localized states with localization length $\ell_c < L$.

Fig. 12 presents the IPR ξ as a function of the quasiparticle energy ϵ and for different system sizes L . All the states are well extended, since there is no size dependence for the quantity $L^2\xi(\epsilon)$, except those in the close vicinity of the Fermi surface ($|\epsilon| < 0.5t$). In the inset of Fig.

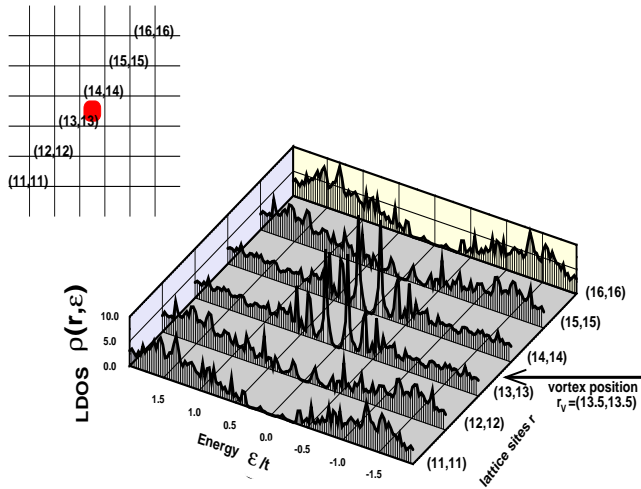


FIG. 14: Quasiparticle local density of states $\rho(\mathbf{r}, \epsilon)$ for the d -wave case at different lattice sites $\mathbf{r} = (11, 11), (12, 12), (13, 13), (14, 14), (15, 15), (16, 16)$ around a vortex position $\mathbf{r}_v = (13.5, 13.5)$ belonging to a regular vortex lattice. The magnetic field is $B = 1/144$. The other parameters are $\Delta_0 = t$ and $\mu = -2.2t$.

12 we present the scaling of the IPR ξ with $1/L^2$. We consider an average over states at the Fermi surface with $|\epsilon| < 0.05t$ (ξ_0 in the inset) and an average over states with $\epsilon \simeq t$ ($\xi_{1.0}$ in the inset). The states close to $\epsilon = t$ are clearly extended since the scaling with $1/L^2$ is quite accurate. The nature of the states close to $\epsilon = 0$ is however less clear. From Fig. 12 we see that the quasiparticle states close to $\epsilon = 0$ deviate from the strict $1/L^2$ scaling law (see the weak intercept of ξ_0 in the inset of Fig. 12), however our results show an obvious size dependence for ξ_0 and do not show a saturation of ξ_0 with the linear system size L . This latter fact indicates, in the hypothesis of an eventual localization of these low-lying states, that we are still far from the thermodynamic limit with the linear system sizes we can currently attain within our model.

To gain further insight into the nature of the low lying states we show in Fig. 13 the LDOS for the states close to $\epsilon = 0$ and those close to $\epsilon = t$. At low energies the LDOS defined by

$$\rho(\mathbf{r}, \epsilon) = \sum_{\mathbf{n}} \left(|u_{\mathbf{n}}(\mathbf{r})|^2 + |v_{\mathbf{n}}(\mathbf{r})|^2 \right) \delta(\epsilon - E_{\mathbf{n}}) \quad (24)$$

is strongly peaked near the vortex cores (upper left panel of Fig. 13). At higher energies ($\epsilon \simeq 1$) the LDOS is much more homogeneously spread over the system indicative of extended states; the values of the LDOS over the lattice are approximatively constant and slightly fluctuate around the expected value for extended states $1/L^2 \simeq 0.0017$ (lower left panel of Fig. 13).

The right side panels of Fig. 13 show the profiles of the internal gauge field \mathbf{a}_s (upper panel) and of the conventional superfluid wave vector \mathbf{k}_s (lower panel) corresponding to the same configuration of vortex pinning as

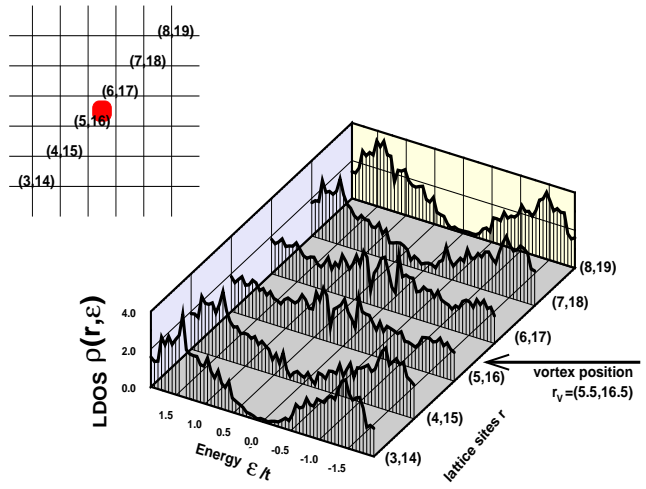


FIG. 15: Quasiparticle local density of states $\rho(\mathbf{r}, \epsilon)$ for the d -wave case at different lattice sites $\mathbf{r} = (3, 14), (4, 15), (5, 16), (6, 17), (7, 18), (8, 19)$ around a vortex position $\mathbf{r}_v = (5.5, 16.5)$ belonging to a disordered vortex lattice. The magnetic field is $B = 1/144$ and we use the 24×24 disordered supercell used in Fig. 13. The other parameters are $\Delta_0 = t$ and $\mu = -2.2t$.

used in the computation of the LDOS (left side panels). For the profile of the superfluid wave vector \mathbf{k}_s the intensity of the supercurrents is peaked around each vortices and rapidly decreases as the inverse of the square of the distance to the vortices. The profile of the internal gauge field \mathbf{a}_s is more interesting. It depicts the two types of vortices A and B whirling in opposite directions (see upper right panel of Fig. 13). Due to this opposite circulation around A - and B -type vortices, the interaction between a A - and a B -type vortex produces significant field currents between the vortices. Fig. 13 shows a spatial correlation between these intervortex currents and the inhomogeneity of the local density of states between the vortices for the low-lying states $\epsilon \simeq 0$ (see upper left panel of Fig. 13).

If we compare now the results for the LDOS with those for the IPR ξ for the low-lying states, we can argue the following: as the participation ratio ξ_0^{-1} physically counts the number of lattice sites occupied by the quasiparticle wave function $\Psi(\mathbf{r})$, and as the low energy states are mainly located around the vortices, the participation ratio ξ_0^{-1} should scale for a fixed magnetic field as the number of vortices in a supercell $\xi_0^{-1} \sim N_\phi \sim BL^2$. This argument explain the fact that ξ_0 in the inset of Fig. 12 seems to follow the $1/L^2$ without saturation, the weak intercept being then negligible. The low-lying quasiparticle states appear then to be delocalized although strongly peaked around the vortex cores.

We present now a spatial scanning of the LDOS in the vicinity of a vortex core for the case of a regular vortex lattice (Fig. 14) and for the case of a disordered vortex lattice (Fig. 15). For both cases the LDOS away from the vortex core are qualitatively the same and are

comparable to that of a d -wave superconductor in a zero-magnetic field. Also for both cases the low-lying states are predominant in the close vicinity of the vortex core but their respective spectra are different. For the regular vortex lattice case (Fig. 14) we remark a double peak structure around the vortex core. This result is in qualitative agreement with the double peak in conductance observed in $\text{YBa}_2\text{Cu}_3\text{O}_{7-\delta}$ by scanning tunneling microscopy (STM)²⁹. For the disordered vortex case (Fig. 15) zero energy peaks (ZEP) appear in the close vicinity of the vortex core (closest neighbor sites) and rapidly disappear (typically over 3δ) when moving away from the vortex core. We note also that close to the vortex cores the coherence peaks disappear in both the regular and the disordered cases.

V. CONCLUSION

In summary, we have calculated the density of states of a disordered superconductor in a pinned fully random vortex array. Both the disorder and the magnetic field fill the density of states at low energies. In the s -wave case the density of states behaves as a power law with an exponent that scales with $1/\sqrt{B}$. In general we find a finite density of states at zero energy for the d -wave case except in the limit of very small magnetic fields. The density of states deviates from the zero energy value by a power law. The zero energy density of states scales with the inverse of the magnetic length (\sqrt{B}). In the d -wave

case the Dirac anisotropy further increases the weight of the density of states at low energies. Also it affects the exponent of the power law. In the isotropic case the exponent is 1 at very low energies and around 2 neglecting this narrow region. In the linear regime the density of states is of the form of a scaling function of the energy and the magnetic field. As the anisotropy increases this narrow regime shrinks considerably and, neglecting this region, the exponent of the density of states interpolates to 1 which is the Dirac limit. This limit is also obtained in the zero field limit in the isotropic case. Except for the zero energy finite value the energy dependence of the density of states in the case with disorder is similar to the lattice case. This suggests that the vortex disorder does not dramatically affect the density of states at low energies. An analysis of the IPR and the LDOS shows that the lowest lying states are delocalized, even though strongly peaked at the vortex cores. In the gapped s -wave case however the disorder introduces states in the gap thereby changing qualitatively the low energy density of states, as in the high field limit¹⁰. We found a power law behavior with an exponent that scales with the magnetic length.

Acknowledgments

This work was supported in part by NSF grant DMR00-94981 (ZT) and by FCT Fellowship SFRH/BPD/5602/2001 (JL).

* Electronic address: lages@cff.ist.utl.pt

† Electronic address: pdss@cff.ist.utl.pt

‡ Electronic address: zbt@pha.jhu.edu

¹ L. P. Gorkov and J. R. Schrieffer, Phys. Rev. Lett. **80**, 3360 (1998).

² P. W. Anderson, cond-mat/9812063.

³ M. Franz and Z. Tešanović, Phys. Rev. Lett. **84**, 554 (2000).

⁴ G. E. Volovik, Pis'ma Zh. Éksp. Teor. Fiz. **58**, 457 (1993); [JETP Lett. **58**, 469 (1993)].

⁵ A. Altland, B. D. Simons, and M. R. Zirnbauer, Phys. Rep. **359**, 283 (2002).

⁶ A. A. Nersesyan, A. M. Tsvelik, and F. Wenger, Phys. Rev. Lett. **72**, 2628 (1994); Nucl. Phys. B **438**, 561 (1995).

⁷ T. Senthil, M. P. A. Fisher, L. Balents, and C. Nayak, Phys. Rev. Lett. **81**, 4704 (1998).

⁸ R. B. Laughlin, Phys. Rev. Lett. **80**, 5188 (1998); T. Senthil, J. B. Marston, and M. P. A. Fisher, Phys. Rev. B **60**, 4245 (1999).

⁹ S. Dukan and Z. Tešanović, Phys. Rev. B **56**, 838 (1997).

¹⁰ P. D. Sacramento, Phys. Rev. B **59**, 8436 (1999).

¹¹ J. Ye, Phys. Rev. Lett. **86**, 316 (2001).

¹² D. V. Khveshchenko and A. G. Yashenkin, cond-mat/0204215.

¹³ J. Lages, P. D. Sacramento, and Z. Tešanović, cond-mat/0301170.

¹⁴ C. Caroli, P. G. de Gennes, and J. Matricon, Phys. Lett. A **9**, 307 (1964).

¹⁵ M. Franz and Z. Tešanović, Phys. Rev. Lett. **80**, 4763 (1998).

¹⁶ O. Vafek, A. Melikyan, M. Franz, and Z. Tešanović, Phys. Rev. B **63**, 134509 (2001).

¹⁷ M. Chiao, R. W. Hill, C. Lupien, B. Popić, R. Gagnon, and L. Taillefer, Phys. Rev. Lett. **82**, 2943 (1999).

¹⁸ J. Lowell and J. B. Sousa, J. Low Temp. Phys. **3**, 65 (1970).

¹⁹ W. A. Atkinson, P. J. Hirschfeld and A. H. MacDonald, Phys. Rev. Lett. **85**, 3922 (2000).

²⁰ M. Franz, C. Kallin and A. J. Berlinsky, Phys. Rev. B **54**, R6897 (1996); M. Franz et al. *ibid* **56**, 7882 (1997).

²¹ A. Ghosal, M. Randeria and N. Trivedi, Phys. Rev. B **63**, 020505 (2000).

²² E. R. Ulm et al., Phys. Rev. B **51**, 9193 (1995); D. N. Basov et al., Phys. Rev. B **49**, 12165 (1994); C. Bernhard et al., Phys. Rev. Lett. **77**, 2304 (1996); S. H. Moffat, R. A. Hughes, and J. S. Preston, Phys. Rev. B **55**, 14741 (1997).

²³ A. Ghosal, M. Randeria, and N. Trivedi, Phys. Rev. Lett. **81**, 3940 (1998).

²⁴ P. I. Soininen, C. Kallin, and A. J. Berlinsky, Phys. Rev. B **50**, 13883 (1994).

²⁵ L. Marinelli, B. I Halperin, and S. H. Simon, Phys. Rev. B **62**, 3488 (2000).

²⁶ A. Vishwanath, Phys. Rev. B **66**, 064504 (2002).

²⁷ Y. Wang and A. H. MacDonald, Phys. Rev. B **52**, R3876

(1995).

²⁸ M. Chiao, R. W. Hill, C. Lupien, L. Taillefer, P. Lambert, R. Gagnon, and P. Fournier, *Phys. Rev. B* **62**, 3554 (2000).

²⁹ I. Maggio-Aprile, Ch. Renner, A. Erb, E. Walker, and Ø. Fischer, *Phys. Rev. Lett.* **75**, 2754 (1995).